PRECISION MEASUREMENT OF THE INCLUSIVE DEEP INELASTIC ep SCATTERING CROSS SECTION AT LOW Q^2

M. KLEIN
for the H1 Collaboration at HERA

Deutsches Elektronen Synchrotron, DESY Zeuthen, Platanenallee 6, D-15738 Zeuthen, Germany
E-mail: klein@ifh.de

A preliminary measurement of the deep inelastic scattering cross section is reported for momentum transfers squared $2 \leq Q^2 \leq 120$ GeV^2 and for Bjorken-x values $3 \cdot 10^{-5} < x < 0.1$. The data were collected by the HERA experiment H1 in 1997, with a luminosity of 15 pb^{-1} for $Q^2 > 10$ GeV^2 and of 2 pb^{-1} taken in a dedicated run for $Q^2 < 10$ GeV^2. This measurement is nearly twice more accurate than results presented previously. It uses in the lower Q^2 region the new Backward Silicon Tracker of the H1 experiment. An analysis of the cross section data combined with fixed target experiments shows NLO QCD to be in very good agreement with the new data. A new method has been developed to determine the longitudinal structure function $F_L(x,Q^2)$ using the derivative $\partial\sigma/\partial \log y$. This permits to access F_L down to low Q^2 values of 3 GeV^2 and leads to results consistent with the method previously used to extract $F_L(x,Q^2)$ at larger Q^2. Data of 4.8 pb^{-1} luminosity taken in 1996 were used for another preliminary measurement of $F_2(x,Q^2)$ in the range $0.2 \leq Q^2 \leq 5$ GeV^2 based on events with a tagged photon from initial state radiation.

1 Cross Section Measurement

The precise measurement of the inclusive neutral current deep inelastic scattering (DIS) cross section $\sigma(ep \rightarrow eX)$ has been one of the prime tasks at HERA as it is required for the understanding of proton substructure and precision tests of QCD. The so-called reduced DIS scattering cross section is defined as

$$\frac{Q^4 x}{2\pi\alpha^2 Y_+} \cdot \frac{d^2\sigma}{dxdQ^2} = \sigma_r = F_2(x,Q^2) - \frac{y^2}{Y_+} \cdot F_L(x,Q^2) \quad (1)$$

with $Y_+ = 1 + (1-y)^2$. For $Q^2 << M_Z^2$ the cross section σ_r is given by the two proton structure functions $F_2(x,Q^2)$ and $F_L(x,Q^2)$ which are related by $0 \leq F_L \leq F_2$. Thus the contribution of F_L is suppressed in most of the kinematic range explored by the H1 experiment and approximately the relation $\sigma_r = F_2$ holds with the exception of the high y region. The measurement presented here[1] is more precise than previous H1 data[2 3 4 5]. New results were obtained on the longitudinal structure function F_L due to an extension of the y range to $y \simeq 0.9$. Further preliminary results[6] on $F_2(x,Q^2)$ were presented, as briefly described in the last section. These are less accurate than the 97 bulk data but reach lowest Q^2 and larger x due to a reduction of the nominal positron beam energy by the measured energy of the photon from initial state radiation (ISR).

1.1 H1 Detector

The H1 detector [7] is a nearly hermetic apparatus with a solenoidal magnetic field of 1.15 T built to investigate high-energy ep interactions at HERA. For polar angles $\theta_e > 153^o$ the scattered positron energy E'_e is measured in the backward electromagnetic lead-fibre scintillator calorimeter (SPACAL [8]) which has an integrated timing function to veto proton beam induced background interactions. Here θ is defined with respect to the proton beam direction. Identification of the scattered positron and the polar angle measurement make use of a backward drift chamber (BDC) and a backward silicon strip detector (BST) situated in front of the SPACAL.

The new BST[9] is a 4 plane silicon strip detector telescope with 64 wedge shaped, single sided, double metal detectors having p$^+$ strips of 96 μm readout pitch arranged concentric around the beam axis to measure the polar angle of crossing tracks for θ between 172^o and 177^o.

The hadronic final state is reconstructed with the Liquid Argon (LAr) calorimeter, the tracking detectors and the SPACAL. The interaction vertex is determined with the central drift chambers, the jet chamber CJC and two layers of z drift chambers, mostly using the hadronic final state particles. This vertex determination is complemented at large Q^2 by the inner proportional chamber CIP and at low Q^2 by the silicon tracker which enables the vertex to be reconstruced at low y using the scattered positron.

The luminosity has been determined to within 1.5% using elastic bremsstrahlung [10]. The final state photon and the positron scattered at very low Q^2 can be detected in calorimeters ("electron and photon taggers") which are situated close to the beam pipe at distances of 33 m and 103 m from the interaction point in the positron beam direction. Part of the photoproduction background events is recognized by tagging the scattered positron in the electron tagger calorimeters upstream the positron beam. This tagged event sample has been essential to understand the background due to very low Q^2 processes.

1.2 *Event Selection and Simulation*

The data are triggered using the local energy sums in the SPACAL calorimeter with an energy threshold set to 5 GeV. A special "high y" trigger down to 2 GeV has been realized by requiring the cluster position in the SPACAL to be above a minimum radius and a valid vertex trigger signature in the proportional chamber system. The efficiency of all trigger elements was larger than 96% and controlled by independent tracking triggers to an accuracy of 0.5-1%.

For the large $Q^2 > 10$ GeV^2 sample the scattered positron was identified as the cluster with maximum transverse momentum p_t. For the low Q^2 sample the scattered positron was considered to be the cluster of maximum energy as at small p_t the fluctuations of the transverse momentum of the hadronic system become more pronounced. The cross section was calculated to be the same within 1-2% when the electron identification criterion was changed and the difference was taken into account in the systematic error. The SPACAL cluster had to be associated with a signal in the preceeding drift chamber (BDC) and, if geometrically available, with a signal in the CIP, for the large Q^2 events, or with a track signature in the BST for the low Q^2 events. For the determination of the event kinematics and background suppression a vertex had to be reconstructed in the CJC, CIP or BST.

The distributions of selected events were compared with simulations of deep inelastic scattering, photoproduction and Compton scattering. The DIS cross section was simulated according to certain parametrization of the parton distributions setting $F_L = 0$. A reweighting procedure was applied using the H1 QCD fit to previous data [5] and calculating F_L to NLO. The simulated Monte Carlo events were submitted to the same reconstruction and analysis chain as the real data. The track detector efficiencies were determined from the data utilizing the redundancy of the central and backward tracking detector system. Agreement at the few per cent level was reached between experiment and simulation for the large set of technical and physics distributions studied.

1.3 *Cross Section*

The cross section is determined by converting the measured number of events, after background subtraction, in a bin averaged cross section using acceptance calculations from the Monte Carlo sample. Due to the imposed requirement on energy-momentum conservation ($E - p_z > 35$ GeV) the radiative corrections are small. The cross section data at large $y > 0.15$ were obtained using the scattered positron angle and energy to reconstruct Q^2_e and y_e. At low $y < 0.15$, where the resolution of y_e degrades, the Σ variables Q^2_Σ and y_Σ were used [11]. The results obtained with the two methods were found to be in excellent agreement down to lowest y which is strong evidence for the correct calibration of the SPACAL energy scale and resolution. All cross section data were obtained in two independent analysis chains.

source	error [%]
positron identification	0.5-2
vertex efficiency	1-2
BDC efficiency	0.5
BST efficiency	1-2
trigger efficiency	0.5 - 1
photoproduction background	< 8 at high y
radiative corrections	1-2
diffractive event simulation	2 at low Q^2, high y
noise rejection in LAr	< 3 at $y < 0.02$
track charge determination	1
charge asymmetry	1
CJC-SPACAL link efficiency	2

Table 1: *Main sources of uncorrelated systematic errors and their effect on the cross section measurement accuracy. The resulting systematic errors are mostly below 4% extending up to 8% at the edges of the covered y range.*

The main sources of uncorrelated systematic errors are summarized in Table 1. The cross section errors due to energy scale and polar angle measurement uncertainties are treated as correlated error sources. The hadronic scale uncertainty is 4/3/5% for the contributions from LAr, tracks and the hadronic energy measurement in SPACAL, respectively. The polar angle error is 0.5 mrad as determined from a comparison of the BDC-vertex with the BST θ measurements. Higher statistics and new instrumentation allowed the systematic uncertainties to be improved by nearly a factor of two as compared to previous H1 results.

1.4 *QCD Analysis*

A NLO QCD fit to the cross section data was performed in the $\overline{MS}$ renormalization scheme using the DGLAP evolution equations for three light flavours with the charm contribution added according to the NLO calculation of the photon-gluon fusion process [12]. The input distributions of $q = g, u_v, d_v$ and S at the starting scale Q^2_o were parametrized as:

$$xq(x) = A_q x^{B_q} (1-x)^{C_q} (1 + D_q x + E_q \sqrt{x}), \qquad (2)$$

where $S = \bar{u} = \bar{d} = 2\bar{s}$ defines the sea distributions. The momentum sum rule was used to fix the normalization parameter A_S and the normalizations of the valence quark distributions were fixed by using the quark counting rules.

The H1 QCD analysis program [13] was extended to fit the inclusive reduced cross section, Eq.(1), and not only its $F_2(x, Q^2)$ part. This avoids the introduction of *ad hoc* assumptions on $F_L(x, Q^2)$ and allows data up to highest y to be included in the QCD analysis. The muon-proton and muon-deuteron DIS cross sections measured by the experiments BCDMS [14] and NMC [15] were also used to constrain the high x behaviour of the parton distributions.

The starting point of the evolution was chosen to be $Q_o^2 = 2$ GeV^2 and data with $Q^2 \geq Q_{min}^2 = 2$ GeV^2 were included in the fit. A cut was made to exclude BCDMS data in the region sensitive to higher twists ($x > 0.5$ for $Q^2 < 15$ GeV^2) and target mass corrections were applied. The strong coupling constant was set to $\alpha_s(M_Z^2) = 0.118$ and the charm quark mass to $m_c = 1.5$ GeV.

In Figure 1 the QCD fit is compared with the cross section data obtained in this measurement. The data are seen to be very well described by the fit to the cross section (solid line). The χ^2 is 1495 for 1095 data points using the uncorrelated errors of the measurements only. The low x behaviour of $F_2(x, Q^2)$ is governed by the parameters B_g and B_S. These depend on Q_o^2 and came out to be equal to -0.18 and -0.14, respectively, for $Q_o^2 = 2$ GeV^2.

At high y the cross section departs from the behaviour of F_2 , dashed line in Figure 1. This departure is due to the longitudinal structure function differing significantly from zero [a].

The fit presented in Figure 1 included the preliminary H1 cross section data measured at high $Q^2 >$ 120 GeV^2 [16] which are very well described. In order to check the predictive power of QCD and the consistency of the two data sets, the cross section fit was repeated excluding the high Q^2 data from the minimization. This leads to a QCD cross section which at $Q^2 = 20000$ GeV^2 agrees within 1-2% with the former one.

2 Cross Section Measurement at Very Large y

2.1 Data Analysis

The measurement of the DIS cross section at HERA at high y requires the scattered positron of a few GeV of energy to be identified and the large background from photoproduction processes to be removed. Since the main part of the background electromagnetic energy deposits is due to $\pi_0 \rightarrow \gamma\gamma$ decays, the low energy background is removed to a large extent by requiring a track pointing to the cluster reconstructed in the SPACAL. At large Q^2 this track is identified with a valid hit pattern in the inner proportional chamber CIP and, for $10 < Q^2 < 40$ GeV^2, as a momentum measured track in the central drift chamber CJC which for energies below 15 GeV identifies the charge.

In the low Q^2 region the high y range was accessed by requiring a track signal in the BST. The largest y cross section data quoted here were obtained in a dedicated analysis which used only the SPACAL and the BST with a minimum bias trigger of 5 GeV threshold. Here the vertex position has been defined only with the positron track candidate passing the BST, and the polar angle measurement of the silicon tracker was used.

2.2 Cross Section Derivative $\partial\sigma_r/\partial \log y$

The cross sections were used to measure the derivative $\partial\sigma_r/\partial \log y$ at fixed Q^2 in the whole y range accessible. This derivative is defined as:

$$\frac{\partial\sigma_r}{\partial \log y} = -\frac{\partial F_2}{\partial \log x} - F_L \cdot 2y^2 \cdot \frac{2-y}{Y_+^2} + \frac{\partial F_L}{\partial \log x} \cdot \frac{y^2}{Y_+}. \quad (3)$$

The data were binned in y and differences $\Delta\sigma_r$ were calculated between all cross section points adjacent in y. A bin center correction was applied to obtain the derivative $\partial\sigma_r/\partial \log y$ at each y point determined as the average of the two y values involved. Contrary to a standard representation of the data, where systematic errors introduce positive correlations between neighbouring points, the two adjacent measurements of $\partial\sigma_r/\partial \log y$ anticorrelate since they contain the same cross section measurement with different sign. Due to the subtraction the systematic errors cancel to a large extent apart from those with a pronounced dependence on y as the photoproduction background at high y and the LAr noise treatment at low y, for example. In Figure 2 the cross section derivative measurement is compared with the NLO QCD calculation using different assumptions on F_L. The derivative is seen to be very sensitive to the longitudinal structure function.

2.3 Longitudinal Structure Function

The measurement of $\partial\sigma_r/\partial \log y$ was used to determine the longitudinal structure function in a new way. In this analysis the assumption has been made that the derivative $\partial F_2/\partial \log y$ is a linear function of $\log y$ up to large y. For all Q^2 straight line fits were made to the derivative data for $y < 0.2$ which describe the data very well. The extrapolation of a straight line was taken to represent the contribution of F_2 at high y. The extrapolations

[a] A QCD fit was also performed to the data restricted to $y < 0.35$ in order to be independent of F_L. It is interesting to notice that this fit and the cross section fit give results for F_2 and F_L which agree within 1% at lowest x for the Q^2 region of this data. Thus the gluon distribution is fixed by the Q^2 dependence of F_2 at lower y, and the influence of F_L on the fit result is small given the presently reached accuracy of the high y cross section measurement.

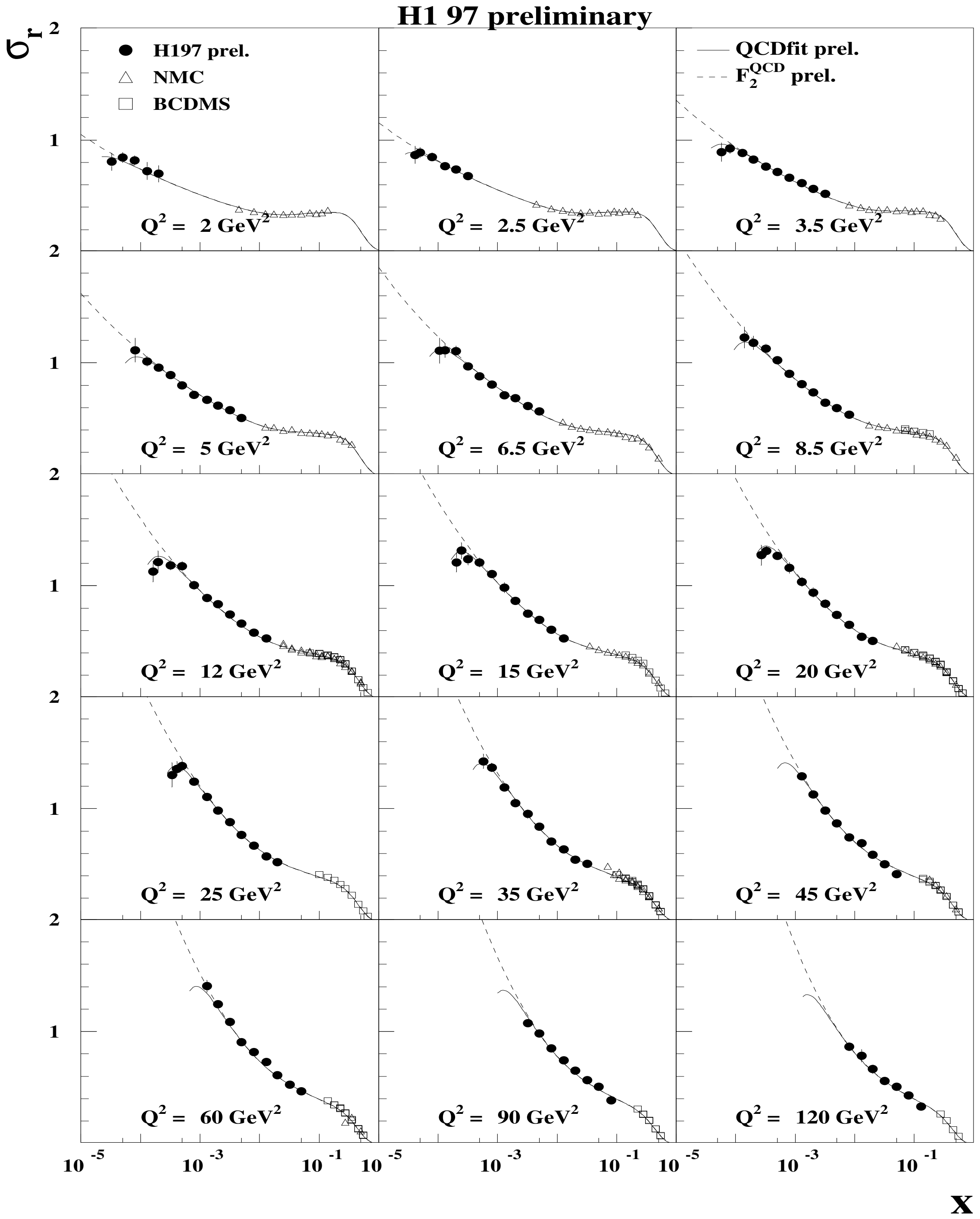

Figure 1: Measurement of the reduced DIS scattering cross section, eq.1, closed points. Triangles (squares) represent data by the NMC (BCDMS) muon proton experiments. The fit is a NLO QCD fit to the H1, the NMC and BCDMS proton and deuteron cross section data as described in the text. The dashed curve is the F_2 structure function determined with this fit. At lowest x, corresponding to large $y \geq 0.5$, departures of the cross section from the rise of F_2 towards low x occur which are mostly due to F_L differing from zero.

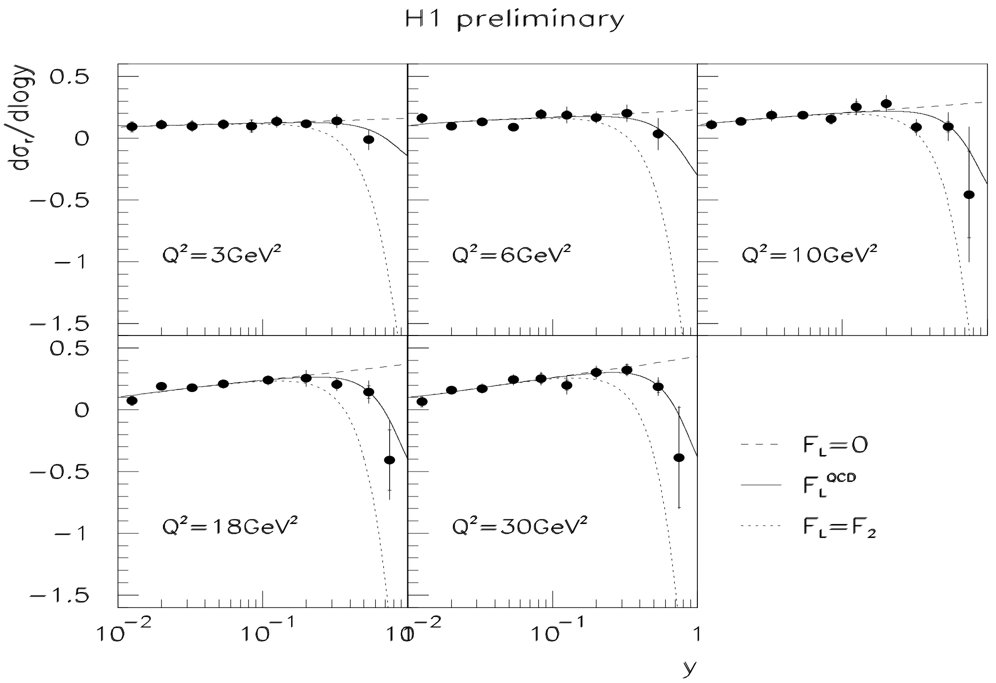

Figure 2: Measurement of the derivative $\partial\sigma_r/\partial \log y$. The curves represent the QCD cross section fit replacing the F_L fit result (solid curve) by $F_L = 0$ (dashed curve) and by $F_L = F_2$ (dotted curve). The inner error bar is the statistical error and the total error bar denotes the statistical and systematic errors added in quadrature.

were compared with the values obtained from QCD and very good agreement was found. The uncertainties of the straight line extrapolation were included into the systematic errors of the measurement. The small contribution of $\partial F_L/\partial \log y$ to the derivative was corrected for by using NLO QCD and the size of the full correction was added to the overall error of the measured F_L.

This procedure leads to new values of F_L (Figure 3). Good agreement is seen with the F_L values derived using the method introduced previously [3] (closed points) which is based on the extrapolation and subtraction of F_2 from σ_r, Eq.(1). All F_L values are consistent with former measurements [3 5]. Both methods use the same data. Yet, the uncertainties of the determined F_L are by construction different. Since at low Q^2 the extrapolation using QCD is uncertain, F_L values down to $Q^2 = 3$ GeV are quoted only using the derivative method. The systematic errors of the $F_L(x, Q^2)$ points are largely correlated as the systematic errors are mainly a function of y in comparable Q^2 intervals.

In Figure 3 bands are drawn which represent the calculation of F_L using the gluon and quark distributions as determined from the NLO QCD fit to F_2 described above. Their width is given by the experimental errors and the uncertainties of α_s and m_c. The data are consistent with this calculation.

3 Tagged Photon F_2 Measurement

The H1 Collaboration has performed a measurement of $F_2(x, Q^2)$ using DIS events with a tagged photon of energy E_γ radiated collinearly to the positron beam. This modifies the event kinematics and permitted the acceptance range of the H1 structure function measurements to be extended towards low $Q^2 \geq 0.2$ GeV^2. The data were collected in 1996 with a luminosity of 4.8 pb^{-1}. Besides the standard DIS event selection cuts with a scattered positron of energy larger than 6 GeV, a photon had to be tagged upstream the positron beam with $E_\gamma > 7$ GeV. Rejection of overlap of events due to elastic bremsstrahlung and inclusive DIS was achieved by requiring no energy in the electron tagger, and the total energy sum had to be conserved. The acceptance and efficiency corrections are based on simulations and on studies using independent detectors, in particular for the trigger efficiencies. The preliminary measurement is shown in Figure 4. The systematic errors are at the 20% level due to energy calibration, vertex reconstruction and radiative correction uncertainties. All data points are obtained using the Σ method for reconstructing the event kinematics apart from the points at lowest x for all Q^2 which are due to the electron method. The $F_2(x, Q^2)$ values agree well with a recent [17] phenomenological description of the transition from DIS to the photoproduction region. In the region of overlap there is good agreement observed of this analysis with the inclusive analysis (Figure 4).

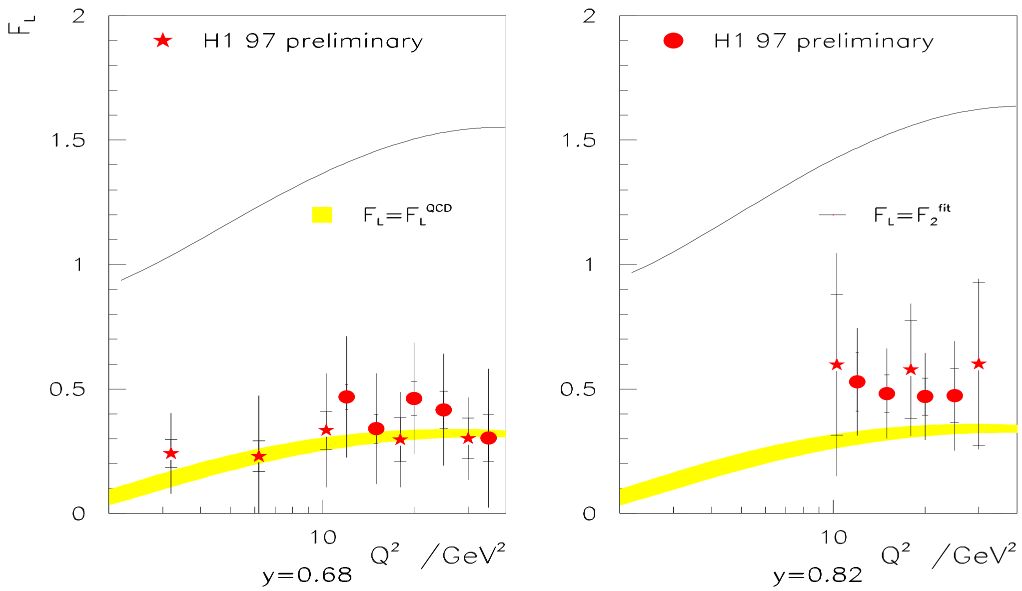

Figure 3: Determination of the longitudinal structure function F_L using the subtraction method (closed points) and the derivative method (stars) which extends to lower Q^2. The quoted y values apply to the closed points. The stars belong to somewhat lower y values as they are derived from a difference of cross section measurements. The two determinations use the same data set. The narrow band represents the uncertainty range of F_L when calculated using the gluon and quark distributions determined with the NLO QCD fit to the H1, NMC and BCDMS data.

4 Summary

A new, preliminary measurement of the deep inelastic positron-proton scattering cross section has been presented based on data taken by the H1 Collaboration at HERA running with positrons of 27.5 GeV energy and with protons of 820 GeV energy. The statistical accuracy of the measured inclusive cross sections is better than 1% for a large part of the data. The systematic precision has reached the level of 3-4% apart from the edges of the covered range. Improvements were due to the higher statistics allowing more refined systematics studies to be performed, and due to the backward silicon tracker for the measurement of low Q^2 scattering. These data represent thus the so far most precise measurement of the proton structure function $F_2(x, Q^2)$ by the H1 Collaboration. They are in agreement with previous results within the quoted systematic accuracy which is now comparable with the precision of fixed target lepton-proton scattering experiments. The behaviour of the DIS cross section was found to be very well described by a NLO QCD analysis which included the data obtained by H1 at even higher Q^2 and by the NMC and BCDMS experiments. All data sets are in good agreement.

The measurement of the cross section at large Q^2 was extended to minimum energies of the scattered positron of 3 GeV. The use of the backward silicon tracker permitted to access the low Q^2, high $y < 0.75$ region with improved precision. This lead to new measurements of the DIS cross section at high y where it is sensitive to the longitudinal structure function $F_L(x, Q^2)$.

A new method was introduced to access, with improved sensitivity, the F_L part of the cross section by measuring the derivative $\partial\sigma_r/\partial \log y$ of the reduced cross section at fixed Q^2. This method profits from a cancellation of systematic errors and has been used to extract $F_L(x, Q^2)$ down to $Q^2 = 3$ GeV at $x \simeq 10^{-4}$. The values of the longitudinal structure function presented here are in good agreement with previous H1 results and consistent with F_L as calculated in the NLO QCD analysis of F_2.

The extended kinematic region $2.2 \cdot 10^{-5} \leq x \leq 0.0032$ and $0.2 \leq Q^2 \leq 5$ GeV^2 was accessed in a smaller data sample, taken in 1996, using DIS events with hard photon radiation collinear to the positron beam. In the region of overlap the radiative analysis is consistent with the inclusive measurement.

Acknowledgements

The 97 data represent the first H1 structure function result obtained with the Backward Silicon Tracker and I would like to thank all my colleagues for their huge efforts to build and operate the BST. The data are due to the success of HERA and the H1 collaboration. Their immediate analysis has been a particular challenge and pleasure shared with enthusiastic young and elder friends. Thanks are due to the radiative group for their help to better understand the merits of the tagged photon analysis of deep inelastic scattering.

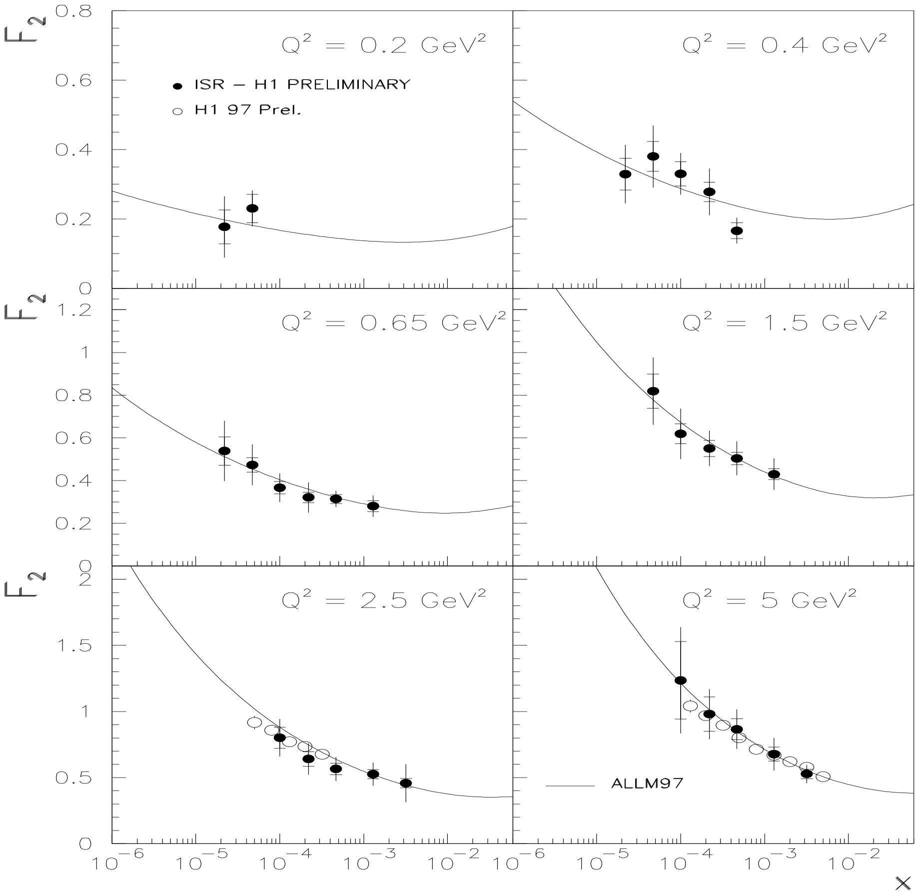

Figure 4: Measurement of $F_2(x, Q^2)$ using tagged photon DIS events. The inner error bars represent the statistical accuracy, the outer bars are the statistical and systematic errors added in quadrature. Open points: standard, inclusive analysis of the 1997 data presented here.

References

1. H1 Collaboration,"Precision Measurement of the Inclusive Deep Inelastic *ep* Scattering Cross Section at Low Q^2", Paper 534, submitted to this Conference, unpublished.
2. H1 Collaboration, S. Aid et al., Nucl. Phys. **B 470** (1996) 3.
3. H1 Collaboration, S. Aid et al., Phys. Lett. **B 393** (1997) 452.
4. H1 Collaboration, C. Adloff et al., Nucl. Phys. **B 497** (1997) 3.
5. H1 Collaboration, Paper 260, submitted to the International Europhysics Conference on High Energy Physics, Jerusalem, Israel, 1997, unpublished.
6. H1 Collaboration, "Low Q^2-Intermediate x Structure Function Measurement at HERA", Paper 535, submitted to this Conference, unpublished.
7. H1 Collaboration, I. Abt et al., Nucl. Instr. and Meth. **A386** (1997) 310 and **A386** (1997) 348.
8. R. Appuhn et al., Nucl. Instr. and Meth. **A 386** (1997) 397.
9. W. Eick et al., Nucl. Instr. and Meth. **A386** (1997) 81.
10. H1 Collaboration, I. Abt et al., Z.Phys. **C66** (1995) 529.
11. U. Bassler and G. Bernardi, Nucl. Instr. Meth. **A361** (1995) 197.
12. S. Riemersma, J. Smith and W. van Neerven, Phys. Lett. **B 347** (1995) 143 and references cited therein.
13. C. Pascaud and F. Zomer, LAL preprint, LAL/95-05 (1995).
14. BCDMS Collaboration, A.C. Benvenuti et al., Phys. Lett. **B223** (1989) 485;
CERN preprint CERN-EP/89-06. Note that the analysis was performed using the data set as modified by M. Virchaux and A. Milzstajn (Phys. Lett. **B274** (1992) 221) to account for systematic effects.
15. NMC Collaboration, M. Arneodo et al., Nucl. Phys. **B483** (1997) 3.
16. M. Fleischer, H1 Collaboration, these proceedings.
17. H. Abramowicz et al., Phys.Lett. **B269** (1991) 465 and hep-ph/9712415.